

RESEARCH ARTICLE

Open Access

Protective role of 1,25(OH)₂vitamin D₃ in the mucosal injury and epithelial barrier disruption in DSS-induced acute colitis in mice

Hongwei Zhao^{1†}, Hong Zhang^{1†}, Hui Wu^{1†}, Hui Li¹, Lei Liu¹, Jian Guo¹, Chenyang Li², David Q Shih³ and Xiaolan Zhang^{1*}

Abstract

Background: Intestinal hyper-permeability plays a critical role in the etiopathogenesis of inflammatory bowel disease (IBD) by affecting the penetration of pathogens, toxic compounds and macromolecules. 1,25-dihydroxyvitamin D₃ [1,25(OH)₂D₃], the active form of vitamin D, has been shown to be an important regulator of IBD and recent epidemiology suggests that patients with IBD have an impaired vitamin D status. The purpose of this study is to investigate the possible protective effects of 1,25(OH)₂D₃ on mucosal injury and epithelial barrier disruption on dextran sulfate sodium (DSS)-induced acute colitis model.

Methods: We used DSS-induced acute colitis model to investigate the protective effects of 1,25(OH)₂D₃ on mucosal injury and epithelial barrier integrity. Severity of colitis was evaluated by disease activity index (DAI), body weight (BW) change, colon length, histology, myeloperoxidase (MPO) activity, and proinflammatory cytokine production including tumor necrosis factor- α (TNF- α) and interferon- γ (IFN- γ). *In vitro* the protective role of 1,25(OH)₂D₃ was assessed by incubating Caco-2 cells with or without DSS and measuring transepithelial electrical resistance (TEER) and fluorescein isothiocyanate dextran (FITC-D). The intestinal permeability was analyzed by FITC-D, bacterial translocation and measurement of lipopolysaccharide (LPS). Ultrastructural features of the colon tissue and Caco-2 cell monolayer were observed by electron microscopy. Expressions of tight junction (TJ) proteins in the colon mucosa and Caco-2 cells were detected by immunohistochemistry, immunofluorescence, Western blot and real-time fluorescent quantitative PCR, respectively.

Results: DSS-induced acute colitis model was characterized by a reduced BW, AUC of BW, serum calcium, higher DAI, AUC of DAI, shortened colon length, elevated MPO activity, worsened histologic inflammation, increased mononuclear cell numbers in mesenteric lymph nodes (MLNs) and colonic lamina propria (LP), and enhanced proteins and mRNA levels of TNF- α and IFN- γ . 1,25(OH)₂D₃ markedly increased expressions of TJ proteins and mRNA and decreased the FITC-D permeability and the level of LPS. Furthermore, 1,25(OH)₂D₃ abrogated bacterial translocation to MLNs and ameliorated ultrastructural features of the colon epithelium by scanning electron microscopy (SEM). *In vitro*, 1,25(OH)₂D₃ increased TEER, TJ proteins and mRNA expressions, decreased the FITC-D permeability, and preserved structural integrity of the TJ in Caco-2 cells.

* Correspondence: xiaolanzh@126.com

†Equal contributors

¹Department of Gastroenterology, The Second Hospital of Hebei Medical University, Hebei Key Laboratory of Gastroenterology, Hebei Institute of Gastroenterology, No.215 Heping West Road, 050000 Shijiazhuang, China
Full list of author information is available at the end of the article

Conclusions: 1,25(OH)₂D₃ may play a protective role in mucosal barrier homeostasis by maintaining the integrity of junction complexes and in healing capacity of the colon epithelium. 1,25(OH)₂D₃ may represent an attractive and novel therapeutic agent for the adjuvant therapy of IBD.

Keywords: Barrier protection function, Dextran sulfate sodium, Inflammatory bowel disease, Tight junction, 1,25-dihydroxyvitamin D₃

Background

Inflammatory bowel disease (IBD), comprised of Crohn's disease (CD) and ulcerative colitis (UC), are chronic diseases characterized by aberrant immune responses to luminal bacteria in genetically susceptible subjects [1]. Although the exact pathogenesis of IBD is unknown, the initiation of inflammation and relapse of disease activity are associated with engagement of the innate and adaptive immune responses, including increased production in tumor necrosis factor- α (TNF- α) and interferon- γ (IFN- γ) in the intestine [2,3]. These pro-inflammatory cytokines are potential pathogenic factors, which impair mucosal barrier function and intestinal permeability. A disproportionate large number of first-degree relatives of patients with IBD have increased intestinal permeability, which suggests barrier dysfunction may be an early defect. Previous studies have demonstrated a decreased expression of junction complex proteins in the intestinal mucosa of patients with IBD [4,5]. Impaired gut epithelial barrier function may lead to persistent immune reactions, thus augmenting the gut inflammation [6].

The intestinal epithelial barrier consists of epithelial cells and intercellular junctions [7-9]. Tight junction (TJ) is the apical-most intercellular structure in epithelial cells, accounting for the cell-cell adhesion, polarity, and permeability barrier to paracellular transport of the solutes [10]. The TJ creates a semipermeable barrier, separating different organ compartments. It is composed of a large number of protein components, such as occludins, claudins and zonula occludens-1 (zo-1). Both claudins and occludins are coupled either directly or indirectly to cytoskeleton actin filaments with zo-1 and other factors. Distributions of claudins vary along the gut epithelial cells and express different types in the connecting cells through the formation of zipper structures [11,12]. Once the mucosal barrier is breached, the sub-mucosa is exposed to a vast pool of luminal antigens, including food and bacteria, and the innate immune responses are engaged to produce large amounts of cytokines. Therefore, maintaining TJ and barrier function may provide potential benefits in the adjuvant therapy of many gastrointestinal diseases, including IBD [13-15].

1,25-dihydroxyvitamin D₃ [1,25(OH)₂D₃], the active form of vitamin D, has been shown to be an important regulator in many experimental autoimmune diseases [16-19]. A recent study has shown that vitamin D directly modulates the T-cell antigen receptor (TCR) [20].

In naive T cells, low expression of phospholipase C (PLC)- γ 1 is correlated with low TCR responsiveness. The induction of PLC- γ 1 was shown to be dependent on vitamin D and vitamin D receptor (VDR) [21]. Studies have implicated that the deficiency of VDR may lead to exaggerated inflammatory responses [22,23]. Consistent with its anti-inflammatory role, 1,25(OH)₂D₃ down-regulates the expressions of many pro-inflammatory cytokines, such as TNF- α , IFN- γ , and other cytokines [24,25]. 1,25(OH)₂D₃ is also important to maintain homeostasis in the respiratory tract, skin, and blood-brain and blood-retinal barrier development. 1,25(OH)₂D₃ has been found to protect the intestinal mucosa from various insults, combination therapy with angiotensin II type 1 (AT II -1). Vitamin D analog markedly restored glomerular filtration barrier structure, and the combined treatment reversed the decline of slit diaphragm proteins, such as nephrin and zo-1. Hence, 1,25(OH)₂D₃ may prevent and treat these conditions [26-28].

The role of 1,25(OH)₂D₃ in the regulation of intestinal barrier integrity and innate immune response in DSS-induced acute colitis is unclear. Herein we hypothesized that 1,25(OH)₂D₃ may play an important role in maintaining the integrity of the intestinal mucosal barrier and regulate the innate immunity, which implicates vitamin D metabolic pathway is a novel target for the adjuvant therapy of IBD.

Methods

Ethics statement

The mice and the protocol involved in the study had been approved by Institutional Animal Care and Use Committee (IACUC). Approval ID: I07-038-3. All the mice were housed under standard conditions per protocols of IACUC and Hebei medical university vivarium in a barrier facility (GB 14925-2001).

Animal studies

C57BL/6 mice were purchased from Vital River Laboratory Animal Technology Co. Ltd for *in vivo* studies [License No. SCXK (Beijing) 2006-0009]. Acute colitis was induced by administration of dextran sodium sulfate (DSS; 40 000-50 000 MW; Sigma) drinking water. Male mice of 8 weeks received either regular drinking water (control) or 2% (w/v) DSS drinking water (model) ad libitum for 7 days, after which the mice were resumed on water for the remainder of the experiment. A total of

30 mice were randomly assigned to control, model and 1,25(OH)₂D₃-treated group (each group = 10). The mice in the 1,25(OH)₂D₃-treated group received 1,25(OH)₂D₃ (Sigma) daily (0.2 ug/25 g/d) by intragastric administration for 14 days [29], and the mice in control and model group were given normal saline without DSS.

Serum measurements

Mice were executed at the end of the experiment. Serum was obtained, and Lipopolysaccharide (LPS) kit was purchased from Sigma, and Calcium (587-A) kit was purchased from Sigma. Serum calcium was measured according to the manufacturer's instructions. Vitamin D deficiency was monitored by serum calcium analysis and normal serum calcium levels for mice are 2.00–2.75 mmol/L [29]. LPS was measured by Limulus quantitative azo color (LQAC) test.

Assessment of disease activity

Rachmilewitz DAI was assessed by an investigator blinded to the protocol according to a standard scoring system. The combined score composes of the extent of body weight (BW) loss, stool consistency and detection of occult blood (OB) in the stool, and they are defined as follows. Loss in BW is scored as: no weight loss is scored as 0, weight loss of 1–5% from baseline as 1, 5–10% as 2, 10–20% as 3, and more than 20% as 4. For stool consistency, a score of 0 is assigned for wellformed pellets, 2 points for pasty and semifformed stools that do not adhere to the anus, and 4 points for liquid stools that were adhere to the anus. For OB, a score of 0 point is assigned for no blood, 2 points for positive hemocult, and 4 points for gross bleeding. These scores are added together and divided by three, resulting in DAI ranging from 0 (healthy) to 4 (maximal activity of colitis) [30] and measured by area under curve (AUC).

Assessment of colonic injury and inflammation

Postmortem, the colon from the cecum to the anus was removed, and the entire colon length was measured as a marker of inflammation. On macroscopic examination, the degree of colon damage was scored as follows: 0, normal colon tissue; 1, minimal colon wall thickening without congestion; 2, moderate colon wall thickening with congestion; 3, moderate colon wall thickening, rigidity, and congestion; and 4, marked colon wall thickening, rigidity, and congestion. A segment of the proximal colon was fixed in 10% formalin, and embedded in paraffin; 4 um-thick sections of this tissue were stained with hematoxylin and eosin (H&E). Histologic evaluation was performed by two investigators blinded to the animal groups and the inflammation was graded as follows: severity of inflammation (0–3: none, slight, moderate, severe), extent of injury (0–3: none, mucosal, mucosal

and submucosal, transmural), and crypt damage (0–4: none, basal 1/3 damaged, basal 2/3 damaged, only surface epithelium intact, entire crypt and epithelium lost). Then each score was multiplied by a equivalent with the percentage of tissue involved (×1: 0–25%, ×2: 26–50%, ×3: 51–75%, ×4: 76–100%).

Determination of myeloperoxidase (MPO) activity

MPO activity in homogenates of the colon was determined in this way: equal weights (100 mg wet weight) of the colon from each group were suspended in 1 mL buffer (0.5% hexadecyltrimethylammonium bromide in 50 mM phosphate buffer, pH 6.0) and sonicated at 30 cycles, twice for 30 s on ice. Homogenates were centrifuged, 2000 g, 4°C, and the supernatants were stored at 80°C. The samples were incubated with a substrate of odianisidine hydrochloride and the reaction was carried out in a 96-well plate by adding to 290 µL 50 mM phosphate buffer, 3 µL substrate solution (containing 20 mg/mL odianisidine hydrochloride), and 3 µL H₂O₂ (20 mM). The samples (10 µL each well) were added to each well to start the reaction. The reaction was stopped by adding 3 µL sodium azide (30%), and the plates were read for the assay at light absorbance of 460 nm. MPO activity was determined by the curve obtained from the standard MPO [31].

Isolation of mesenteric lymph nodes cells (MLNs) and lamina propria mononuclear cells (LPMCs)

Mesenteric lymph nodes (MLNs) were placed in a petri dish with 2 mL ice-cold RPMI 1640. Two prewet sterile glass slides were used to smash MLNs, and then passed through a 70 µm nylon cell strainer into a 50 mL Falcon tube. Petri dish and glass slides were rinsed with an additional 3 mL RPMI 1640, centrifuged, removed the supernatant, and resuspended the pellet in 1.0 mL RPMI 1640 with 10% FCS. The cells were then counted. Isolation of lamina propria mononuclear cells (LPMCs) was described as follows: The dissected gut was opened longitudinally, transferred onto HBSS/5 mM EDTA and incubated for 20 min at 37°C under slow rotation (40 g) in a thermal incubator. Gut tissues were then transferred onto a new petri dish with 1–2 mL collagenase solution (100 mL of RPMI 1640 with 10% FCS [32]: Hyaluronidase, 0.25 g; Collagenase type II, 0.15 g; DNase I, 0.025 g) and minced into about 1 mm-square pieces. The minced tissues were then passed through a 70 um cell strainer, then centrifuged, resuspended the pellet in 6 ml of 45% Percoll solution, overlaid the cell suspension on top of 3 mL of the 72% Percoll solution, centrifuged, carefully collected the cells, centrifuged again, aspirated and resuspended the cells immediately in 500 µL RPMI 1640 with 10% FCS, and at last counted cells one by one [33].

Immunohistochemistry/immunofluorescence

For immunohistochemistry staining, antigens were retrieved by 10 min boiling in 10 mM citrate (pH 6.0). The slides were stained with mouse monoclonal anti-claudin-1 antibody, anti-occludin antibody (Santa Cruz), and rabbit polyclonal anti-zo-1 antibody (Invitrogen), rabbit polyclonal anti-IFN- γ antibody (Santa Cruz) and mouse monoclonal anti-TNF- α antibody (sigma). After incubation with peroxidase-conjugated secondary antibody, signals were visualized with a diaminobenzidine (DAB) peroxidase substrate kit (Vector Laboratories). For TJ immunofluorescence staining, Caco-2 cell monolayer (fixed in 95% ethanol) or colon sections were incubated with mouse monoclonal anti-claudin-1 antibody, anti-occludin antibody (Santa Cruz) and rabbit polyclonal anti-zo-1 antibodies (Invitrogen), then with an FITC-conjugated secondary antibody or Cy3-conjugated secondary antibody. Slides were examined with a Leica DMIRE2 scanning laser confocal microscope.

In vivo permeability

In vivo permeability assay was performed to assess barrier function and performed by fluorescein isothiocyanate dextran (FITC-D). Briefly, food and water were withdrawn for 4 h, and mice were gavaged with permeability tracer (60 mg/100 g BW of FITC-D (MW 4 000; Sigma). Serum was collected retroorbitally 4 h after FITC-D gavaged, and fluorescence intensity was measured (excitation, 492 nm; emission, 525 nm; Cytofluor 2 300 nm; Millipore), and FITC-D concentrations were determined from standard curves generated by serial dilution of FITC-D [34]. Permeability was calculated by linear regression of sample fluorescence (Excel 5.0, Microsoft Office). Detection of viable bacteria in MLNs represented bacterial translocation from the lumen to the MLNs. The MLNs of left colonic regions were removed aseptically and dissected free of fat. A 0.1 ml aliquot of each homogenate was plated into blood agar, incubated at 37°C for 48 h, and then counted the number of colonies. The ratio of bacterial translocation was presented for percentage.

Electron microscopy

Specimens were fixed, washed in acetone, critical point dried, coated with gold by a sputter coater, and observed under scanning electron microscope (SEM) fitted with a lanthanum hexaboride cathode using an accelerating voltage of 10 kV. Cell monolayer samples were fixed in 2% glutaraldehyde and postfixed in 1% osmium tetroxide in 0.1 M phosphate buffer, pH 7.4, 1 h, 37°C. The tissues were dehydrated in an ascending series of ethanol, infiltrated with eponate 12 resin and then embedded and polymerized, 70°C, 24 h. Resin-embedded blocks were sectioned at 70 nm and collected on 200 mesh, formvar-

coated copper grids. Grids were stained with uranyl acetate and lead citrate and examined with a JEOL 1200 EX II transmission electron microscope (TEM).

Caco-2 cell culture

The Human Colon Carcinoma cell Line (Caco-2) was purchased from Shanghai Institutes of Biochemistry and Cell Biology for *in vitro* studies, and cultured in medium supplemented with 10% fetal bovine serum (FBS) and penicillin (50 U/ml)/streptomycin (50 μ g/mL) in a 5% CO₂ atmosphere at 37°C. Caco-2 cell monolayer was incubated with or without 2% DSS in the absence or presence of 10⁻⁹, 10⁻⁸, 10⁻⁷ M of 1,25(OH)₂D₃ (administered 2 h prior to DSS) for 48 h.

In vitro permeability

Paracellular permeability was determined by measuring the apical to the basolateral flux of FITC-D using a modification of previously described method [34]. Briefly, confluent epithelial monolayer on a 0.33 cm², 0.4 μ m pore size permeable support was washed twice with Hanks' balanced salt solution containing calcium chloride and magnesium sulfate (HBSS) and maintained at 37°C on a shaking warm plate. FITC-D, 1 mg/mL, was added apically at time 0, and 50 μ L samples were removed from the basolateral compartment at 30 min intervals from 0–360 min, inclusively. Fluorescence intensity of each sample was measured (excitation, 492 nm; emission, 525 nm; Cytofluor 2 300 nm; Millipore Corp, Waters Chromatography, Bedford, MA), and FITC-D concentrations were determined from standard curves generated by serial dilution of FITC-D. Paracellular flux was calculated by linear regression of sample fluorescence (Excel 5.0, Microsoft WA, Power Macintosh 7200).

TEER measurement

For transepithelial electric resistance (TEER) measurement, Caco-2 cells were cultured on collagen-coated transwell polycarbonate membrane filter inserts (Corning). The cells were seeded at a density of 1 \times 10⁵ cell/mL, the medium was changed every 1 or 2 days. The integrity of the monolayer was observed to accomplish after culturing for 21 days, and evaluated by measuring TEER with Millicell-Electrical Resistance System (ERS) equipment (Millipore). Monolayer showing TEER values of 130–200 ohm/cm² were used for the experiments. The monolayer cells were gently rinsed three times with HBSS and equilibrated in the same solution for 30 min at 37°C (inside volume; 400 μ L, outside volume; 600 μ L). An aliquot (40 μ L) of the apical solution was replaced by the same volume of sample solution, containing each compound at concentrations of 100–800 μ g/mL, and the TEER value of the monolayer was monitored for up to 360 min after adding to the sample solution [35].

Real-time fluorescent quantitation PCR (real time Q-PCR)

The expressions of the gene zo-1, occludin, claudin-1, TNF- α and IFN- γ were characterized by real time Q-PCR. Briefly, Total RNA was extracted from colons or Caco-2 cells using Trizol (Gibco) reversely transcribed into cDNA according to manufacture's protocol. The primers for the zo-1, occludin and claudin-1 genes were as follows: zo-1-Forward 5'-TCATCCCAAATAAGAACAGAGC-3', zo-1-Reverse 5'-GAAGAACAACCCTTTCATAAGC-3', (198 bp amplicon); occludin-Forward 5'-CTTTGGCTACGGAGTGGCTAT-3' occludin-Reverse 5'-CTTTGGCTGCTCTTGGGTCTG-3', (86 bp amplicon); Claudin-1-Forward 5'-GCTGGGT-TTCATCCTGGCTTCT-3', Claudin-1-Reverse 5'-CCTGAGCGGTCACGATGTTGTC-3', (110 bp amplicon); GAPDH-Forward 5'-GAGACCTTCAACACC CCAGC-3', GAPDH-Reverse 5'-ATGTCACGCACGATT TCCC-3', (263 bp amplicon); IFN- γ -Forward 5'-ATGAA CGCTACACACTGCATCTT-3' IFN- γ -Reverse 5'-TTTC TTCCACATCTATGCCACTT3' (139 bp amplicon); TNF- α -Forward 5'-GGTTCTGTCCCTTTCACACTACT-3' TNF- α -Reverse 5'-GAGAAGAGGCTGAGACATAGGC-3' (169 bp amplicon). Reaction system: 10 μ L 2.5 \times Real master Mix, 1.25 μ L 20 \times SYBR solution, 0.5 μ L upstream primer, 0.5 μ L downstream primer and 2 μ L DNA template was brought up to 25 μ L with purified water. The amplification was performed with Quantitect[™] SYBR[®] Green PCR Mastermix (Qiagen), using the following time and temperature profile: 95°C for 5 min, 45 cycles of 1 min at 95°C, 10 s at 60°C. Fluorescent quantitative analysis was performed with the thermal cycler's software package to calculate the Δ Ct value. The levels of zo-1, occludin, claudin-1, TNF- α and IFN- γ were calculated by the $2^{-\Delta\Delta$ Ct analysis. The $2^{-\Delta\Delta$ Ct was presented as the relative expression of the gene expression.

Western blot analysis

The concentration of proteins of colon tissue and caco-2 cells were determined using coomassie brilliant blue assay, the extracts containing equal quantities of proteins (100 μ g) were electrophoresed in 8% polyacrylamide gel. Subsequently, the separated proteins were transferred onto a nitrocellulose membrane. The membrane was blocked for non-specific binding for 30 min (5% skimmed milk in PBS), and then incubated overnight at 4°C with rabbit anti-zo-1 polyclonal antibody (1:100), mouse anti-claudin-1 monoclonal antibody (1:200), anti-occludin antibody (1:200), rabbit polyclonal anti-IFN- γ antibody (1:200), mouse monoclonal anti-TNF- α antibody (1:200) and rabbit anti-GAPDH monoclonal antibody (1:100). The membrane was subsequently incubated at room temperature for 2 h with goat anti-rabbit IgG (1:2 000)/anti-mouse IgG (1:2 000). Blots were developed with enhanced chemiluminescence detection reagents (Santa Cruz Biotechnology Inc),

exposed on Kodak Xmat blue XB-1 film and quantified by Bandscan 5.0 software using GAPDH as internal control. Densitometry is reported using the integral optical density value (IOD). The results were represented in the form of IOD ratio of the target protein to GAPDH.

Statistical analysis

Data were expressed as mean \pm standard deviation (mean \pm SD) and analyzed with SPSS 13.0 software. The comparison of mean variability among all the groups was conducted by one-way ANOVA analysis and two group comparison with LSD test. A Student's *t*-test was carried out for independent samples. Statistical significance was considered at $P < 0.05$.

Results

1,25(OH)₂D₃ ameliorated clinical symptoms of established acute colitis model

As expected, the serum calcium concentrations in model group (1.74 \pm 0.07) mmol/L was lower than that in control group (2.35 mmol/L \pm 0.06 mmol/L, $P < 0.01$) and in 1,25(OH)₂D₃-treated group (2.60 mmol/L \pm 0.07 mmol/L, $P < 0.01$). DSS caused the damage of the colon mucosal barrier, leading to gut inflammation and weight loss. We observed that mice in the model group had significantly greater weight loss than that in the control group from day 3 to day 8. Mice in 1,25(OH)₂D₃-treated group had similar degree of weight loss as mice in the model group from day 3 to day 8. However, mice in the 1,25(OH)₂D₃-treated group had rapid weight recovery from day 9 to day 21 than those in the model group (Figure 1A) and the AUC of BW in the model group was smaller than that in the control group (1841.75 \pm 52.11 vs 2195.60 \pm 21.26, $P < 0.01$) and in the 1,25(OH)₂D₃-treated group (1841.75 \pm 52.11 vs 1902.64 \pm 31.61, $P < 0.01$). Similarly, mice in the 1,25(OH)₂D₃-treated group had firmer stool and less blood in the stool than those in the model group from day 9 to day 21. DAI, consisting of weight loss, stool consistency and OB, were measured daily, and the percentage of weight change of model group was shown in Figure 1B and the AUC of DAI in model group was larger than that in the control group (43.78 \pm 8.95 vs 0.00 \pm 0.00, $P < 0.01$) and in the 1,25(OH)₂D₃-treated group (43.78 \pm 8.95 vs 32.52 \pm 6.49, $P < 0.01$).

1,25(OH)₂D₃ inhibited colonic inflammation

Mice in the model group had significantly worse macroscopic inflammation than those in the 1,25(OH)₂D₃-treated group (Figure 1C and D). Colon shortening was used as a marker of inflammation. Consistent with the macroscopic inflammatory score, we found that by day 8, the colon length, in the model group was shorter than that in the control group (4.88 \pm 0.63 cm vs 6.80 \pm 0.27 cm, $P < 0.01$) and in the 1,25(OH)₂D₃-treated

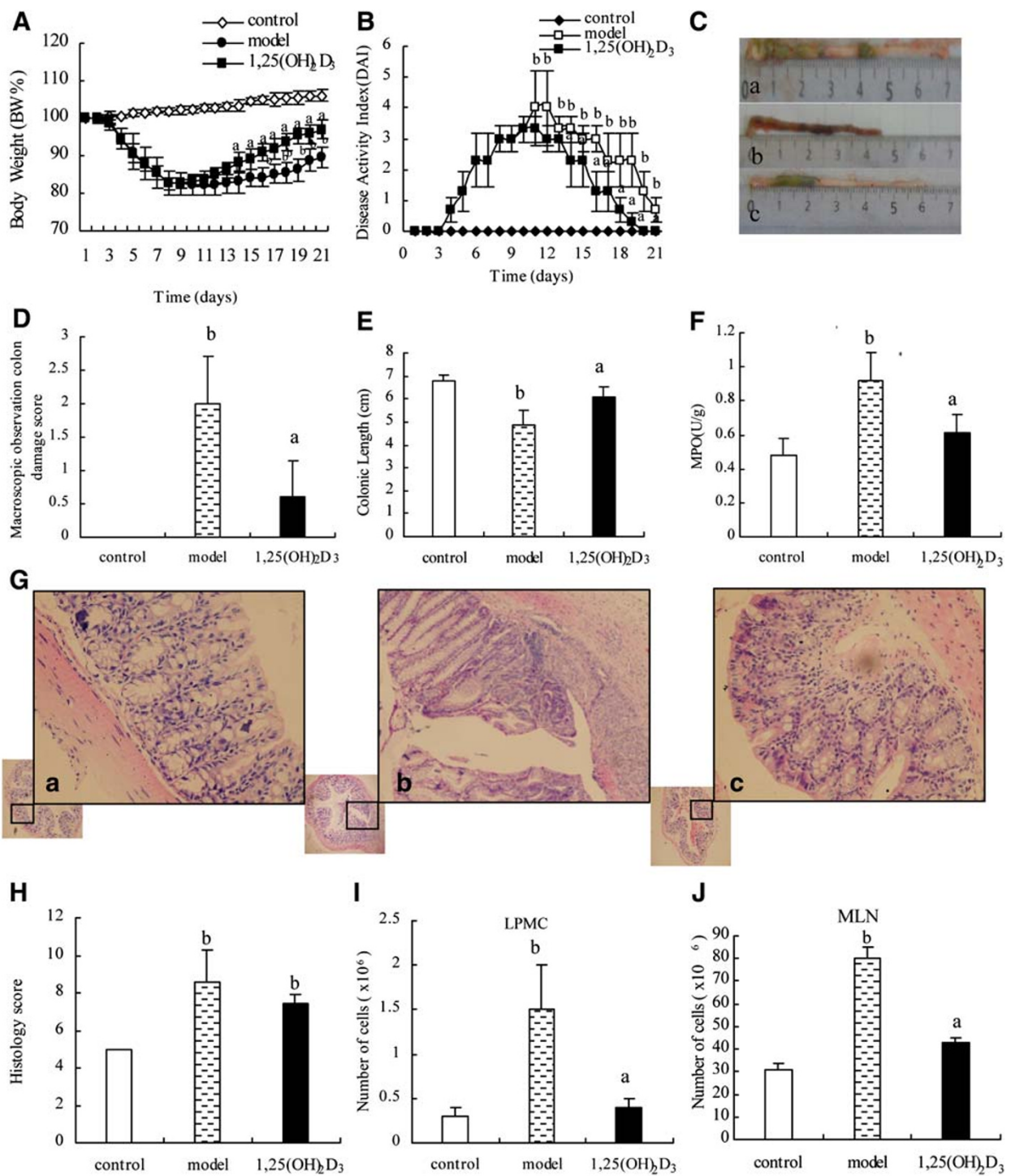


Figure 1 The inflammation in the DSS-induced model of acute colitis. **(A)** BW, shown as percentage of weight change, was assessed daily and represented from day 0 to day 21. Compared to the control group, the model group displayed a more weight loss of BW. **(B)** DAI, comprised of weight loss, stool consistency and OB, was shown. **(C)** Representative photographs of colon at the end of experiment were shown for control group **(a)**, model group **(b)**, and 1,25(OH)₂D₃-treated group **(c)**. **(D)** Macroscopic inflammation was assessed and shown. **(E)** The length of the colon was quantitated and shown. **(F)** MPO enzymatic activity was measured and shown. **(G)** Representative H&E stained histology from control group **(a)**, model group **(b)** and 1,25(OH)₂D₃-treated group **(c)** (H&E staining; original magnifications, ×200). **(H)** Colon histological scores in control, model and 1,25(OH)₂D₃-treated group were shown. **(I and J)** The total number of mononuclear cells from MLNs and LP was more in the model group compared with that in the control group. Data were expressed as mean ± SD. ^aP < 0.01 vs model group; ^bP < 0.01 vs control group.

group (4.88 ± 0.63 cm vs 6.10 ± 0.42 cm, $P < 0.01$) (Figure 1E). In addition, mice in the model group had significantly higher MPO activity than those in the $1,25(\text{OH})_2\text{D}_3$ -treated group (0.92 ± 0.16 vs 0.61 ± 0.11 , $P < 0.01$) and the control group (0.92 ± 0.16 vs 0.48 ± 0.10 , $P < 0.01$) (Figure 1F).

Compared to the control group, histological examination of the colon in the model group showed extensive ulceration of the epithelial layer, edema, crypt damage of bowel wall, fibrosis of the muscularis mucosae, infiltration of granulocytes and mononuclear cells into the mucosa. Compared to mice in the model group, the mice treated with $1,25(\text{OH})_2\text{D}_3$ had a reduced DSS-induced histologic colitis (Figure 1G). Histologic score includes: severity of inflammation, extent of injury, crypt damage, each score was multiplied by a factor equivalent with the percentage of tissue involvement, then the histology score is the sum of all parts of score. Our data showed that histology score in the model group had significantly higher than that in the control group (8.60 ± 2.20 vs 5.00 ± 0.00 , $P < 0.01$), however, histology score in the $1,25(\text{OH})_2\text{D}_3$ -treated group had no significantly lower than that in the model group (7.40 ± 0.80 vs 8.60 ± 2.20 , $P > 0.05$) (Figure 1H). The number of mononuclear cells from the MLNs and LP was more in the model group than that in the control group (MLNs: $80.33 \times 10^6 \pm 14.51 \times 10^6$ vs $30.67 \times 10^6 \pm 3.06 \times 10^6$, $P < 0.01$; LPMC: $1.5 \times 10^6 \pm 0.5 \times 10^6$ vs $0.3 \times 10^6 \pm 0.1 \times 10^6$, $P < 0.01$). Compared to mice of the model group, mice treatment with $1,25(\text{OH})_2\text{D}_3$ reduced the number of mononuclear cells from the MLNs and LP (MLNs: $42.67 \times 10^6 \pm 2.52 \times 10^6$; LP: $0.4 \times 10^6 \pm 0.1 \times 10^6$, $P < 0.01$) (Figure 1I and J). To determine the anti-inflammatory effect of $1,25(\text{OH})_2\text{D}_3$ on the DSS-induced colitis, inflammatory markers were used for immunohistochemistry including TNF- α and IFN- γ on colon tissues in the control group (Figure 2A a and Figure 2B a), the expressions of the TNF- α and IFN- γ were not seen and there were significantly increased expressions of the TNF- α and IFN- γ in the model group (Figure 2A b and Figure 2B b) than those in the $1,25(\text{OH})_2\text{D}_3$ -treated group (Figure 2A c and Figure 2A c). The protein levels of these inflammatory cytokines in the model group were higher than those in the control group by Western blot (TNF- α : 0.69 ± 0.04 vs 0.54 ± 0.03 , $P < 0.01$; IFN- γ : 0.64 ± 0.03 vs 0.33 ± 0.03 , $P < 0.01$) and in the $1,25(\text{OH})_2\text{D}_3$ -treated group (TNF- α : 0.69 ± 0.04 vs 0.63 ± 0.04 , $P < 0.01$; IFN- γ : 0.64 ± 0.03 vs 0.55 ± 0.02 , $P < 0.01$) (Figure 2C and D). Mice treated with $1,25(\text{OH})_2\text{D}_3$ had reduced mRNA levels of inflammatory cytokines when compared to those in the model group (TNF- α : 4.48 ± 0.08 vs 8.34 ± 0.11 , $P < 0.01$; IFN- γ : 8.5 ± 0.34 vs 14.18 ± 0.86 , $P < 0.01$) (Figure 2E). Together, these data indicated that $1,25(\text{OH})_2\text{D}_3$ may ameliorate the inflammation in the colitis model.

$1,25(\text{OH})_2\text{D}_3$ attenuated the DSS-induced paracellular permeability

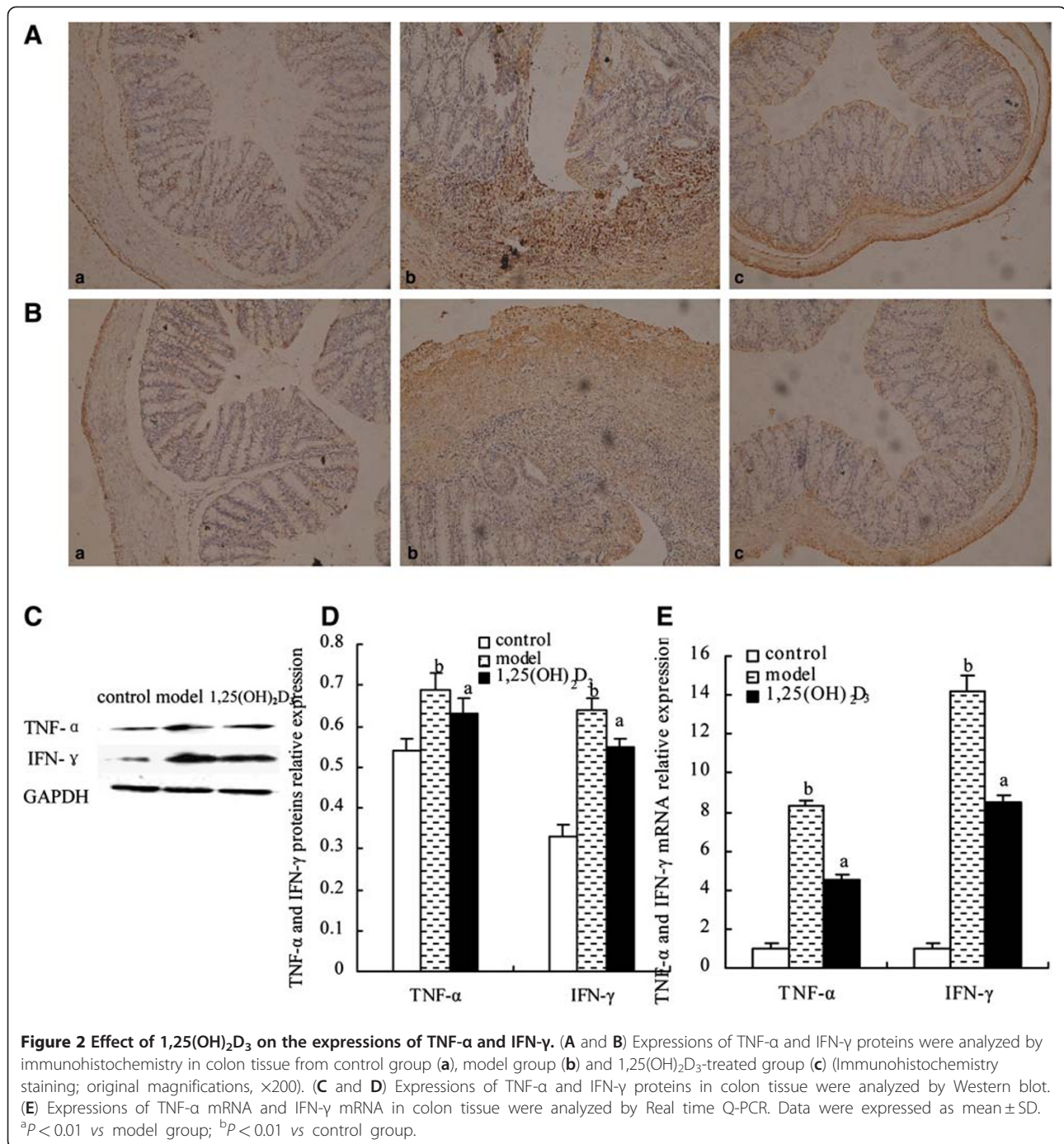
To investigate the effect of $1,25(\text{OH})_2\text{D}_3$ on paracellular permeability, we examined intestinal permeability in animals subject. One of measures of permeability was bacterial translocation. Our study showed $1,25(\text{OH})_2\text{D}_3$ significantly reduced bacteria translocation to the MLNs in the $1,25(\text{OH})_2\text{D}_3$ -treated group when compared to the model group (Figure 3A and B). Another measure of intestinal permeability was FITC-D permeability. Our data showed that the mice in the $1,25(\text{OH})_2\text{D}_3$ -treated group had a lower intestinal permeability to 4-kDa FITC-D when compared to that in the model group (Figure 3C). Consistent with reduced bacterial translocation, there was a result that the blood LPS levels in the $1,25(\text{OH})_2\text{D}_3$ -treated group was lower than that in the model group (Figure 3D). These results suggested that $1,25(\text{OH})_2\text{D}_3$ may maintain intestinal epithelial integrity by decreasing paracellular permeability.

$1,25(\text{OH})_2\text{D}_3$ ameliorated DSS induced ultrastructural changes

SEM was used to observe ultrastructural features of the colon in different groups. We found that the colon in the model group had severer loss of the mucosa with typical histological inflammation, including crypt distortion compared to that in the control group (Figure 3E a, b). Additionally, a greater number of enterocytes from the mice in the model group (Figure 3E c, d) showed less of the glycocalyx, and more irregular of the surface than that in the control group. Meanwhile, mice treatment with $1,25(\text{OH})_2\text{D}_3$ showed ameliorated ultrastructural changes (Figure 3E e, f). These data suggest that $1,25(\text{OH})_2\text{D}_3$ may reduce intestinal permeability in part by preserving ultrastructural integrity of the epithelial mucosa.

$1,25(\text{OH})_2\text{D}_3$ prevented DSS-induced disruption of TJ

TJ complexes interact with the actin cytoskeleton at the apical end of the lateral membranes. To determine the protective effect of $1,25(\text{OH})_2\text{D}_3$ on the DSS-induced disruption of TJ, TJ markers were used for immunohistochemistry including zo-1, occludin and claudin-1 on colon epithelium. In the control group, TJ proteins were seen on the cellular membrane of the epithelial cells, mostly in the spinous and granular layers. In the $1,25(\text{OH})_2\text{D}_3$ -treated group, the expression of the TJ increased in both the cellular membrane and cytoplasm of spinous and granular layers in the mucosa. However, in the model group, expressions of the TJ decreased in individual cells of the spinous and granular layers (Figure 4A and B). To determine whether $1,25(\text{OH})_2\text{D}_3$ could prevent DSS-induced reduction in TJ expression, we performed real time Q-PCR analysis for TJ markers message levels (Figure 4C). We demonstrated that



when compared to TJ expressions in control group, in the model group there were a significantly reduced expressions in zo-1, occludin and claudin-1 (0.46 ± 0.03 vs 1 ± 0.07 , 0.36 ± 0.02 vs 1.00 ± 0.04 , 0.85 ± 0.05 vs 1.00 ± 0.05 , respectively; $P < 0.01$). We also found that TJ marker expressions in the 1,25(OH)₂D₃-treated group were also significantly higher than that in the model group (zo-1: 0.97 ± 0.04 , occludin: 0.98 ± 0.01 , claudin-1: 1.00 ± 0.04 ; $P < 0.01$) (Figure 4D and E), which suggested the importance of

1,25(OH)₂D₃ to maintain the integrity of the junction complex.

The effect of 1,25(OH)₂D₃ on the structure and function of the junction complexes *in vitro*

To further address molecular mechanisms of the protective role of 1,25(OH)₂D₃ in intestinal barrier function, we used an established *in vitro* Caco-2 cells culture system. Caco-2 cells formed TJ when grown to monolayer

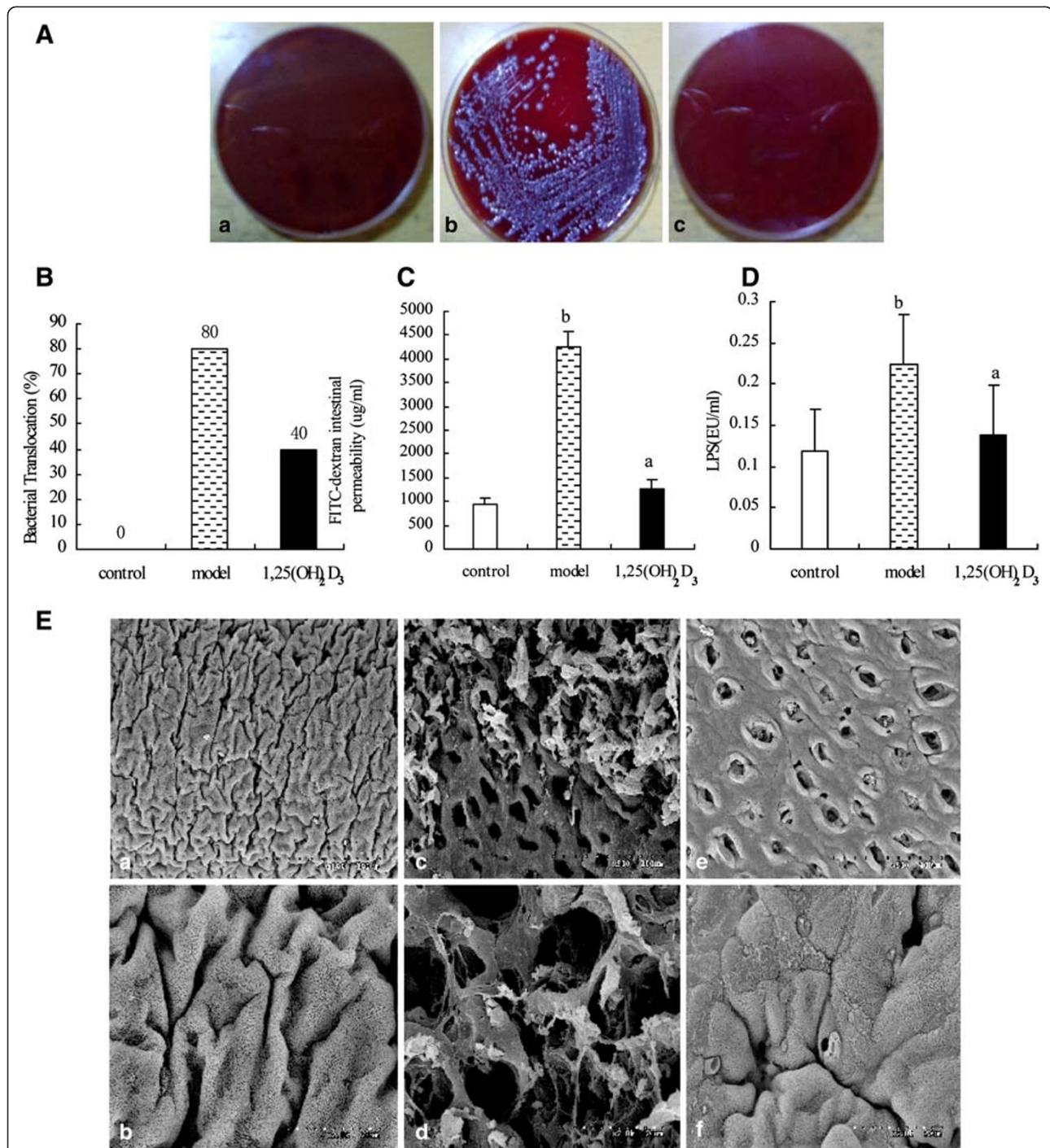


Figure 3 1,25(OH)₂D₃ attenuated the loss of intestinal barrier during DSS-induced colitis model. (A) Detection of viable bacteria in MLNs were shown for control group (a), model group (b) and 1,25(OH)₂D₃-treated group (c). (B) Differences in incidence of bacterial translocation were quantitated and shown, (C) Quantification of serum FITC-D, a measure of intestinal barrier function, was shown. (D) The levels of endotoxin were compared between control group, model group and 1,25(OH)₂D₃-treated group. Data were expressed as mean ± SD. ^a*P* < 0.01 vs model group; ^b*P* < 0.01 vs control group. (E) The ultrastructural features were observed by SEM. The colon mucosa in the control group was regular without histological lesion, (a, ×500; b, ×2 000); In the model group, the mucosa was severe loss, with histological lesions including crypt distortion and abscesses, (c, ×500; d, ×2 000); Areas with histological lesions in the 1,25(OH)₂D₃-treated group were significantly ameliorated; However, compared with the control group, there were less lesions and the crypt distortion and abscesses were less severer. Furthermore, crypt openings were disposed in rows. (e, ×500; f, ×2 000).

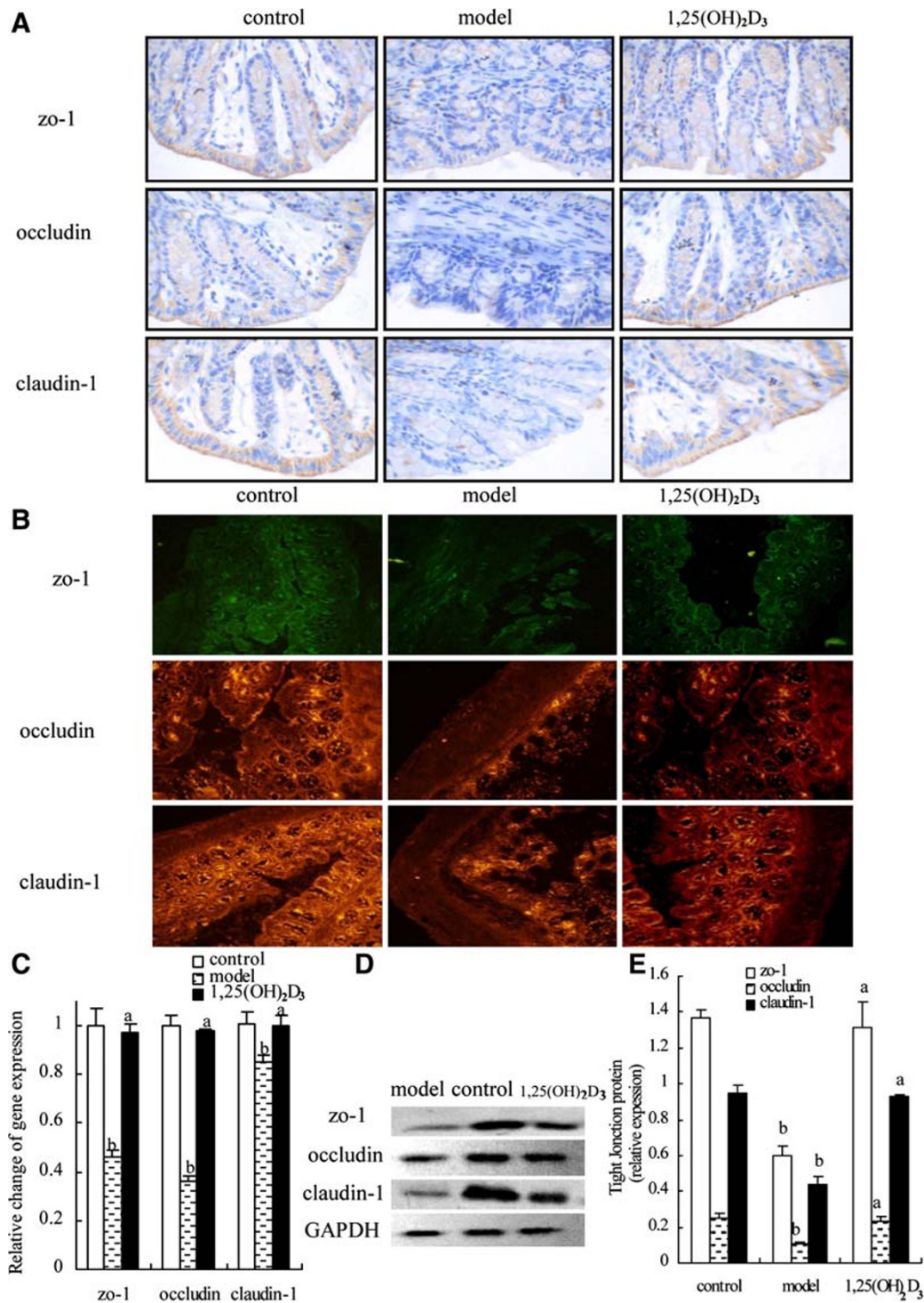


Figure 4 Effect of 1,25(OH)₂D₃ on colonic epithelial junctions. (A) Expressions of zo-1, occludin and claudin-1 were examined by immunostaining for control, model, and 1,25(OH)₂D₃-treated group. Magnification: ×200. (B) Immunofluorescent stain with anti-claudin-1 (red), anti-occludin (red) and anti-zo-1 (green) antibody was shown. Notes of the zo-1, occludin and claudin-1 staining were markedly decreased in the model group compared with that of the control and 1,25(OH)₂D₃-treated group. (C) Expressions of zo-1, occludin and claudin-1 genes were performed and shown by real time Q-PCR analysis. (D and E) Expressions of TJ proteins in the colon were assessed by Western blot. In model group, expressions of zo-1, occludin and claudin-1 were decreased markedly compared with that of control group. Data were expressed as mean ± SD. ^a*P* < 0.01 vs model group; ^b*P* < 0.01 vs control group.

on membrane filters. As in the case of Caco-2 cells, the addition of $1,25(\text{OH})_2\text{D}_3$ to the Caco-2 cells for 48 h increased levels of TJ proteins and mRNA such as zo-1, claudin-1, and occludin, and the optimum dose occurred at 10^{-8} M (Figure 5A, B and C). Further examination of these Caco-2 cell monolayer with TEM revealed intact TJ, desmosomes, microvillus and brush border on the apical side of Caco-2 cell monolayer in the $1,25(\text{OH})_2\text{D}_3$ -treated group (Figure 5D). Consistently, immunostaining with anti-zo-1, claudin-1, and occludin antibodies showed that $1,25(\text{OH})_2\text{D}_3$ (10^{-8} M) markedly enhanced TJ expression in the Caco-2 monolayer, and reflected by bright staining in the membranes of the treated cells. When the cells were incubated with 2% DSS for 2 h, the TJ on the monolayer was markedly disrupted. In contrast, in the presence of $1,25(\text{OH})_2\text{D}_3$, the TJ was resistant to the DSS damage and remained intact, as evidenced by a strong staining of the zo-1, claudin-1, and occludin on the membranes between the cells (Figure 5E). When Caco-2 monolayer was incubated with 2% DSS, the TEER gradually decreased over 6 h in the DSS group. However, in the $1,25(\text{OH})_2\text{D}_3$ -treated cells, the TEER was moderately reduced over the following 6 h (Figure 5F). Interestingly, FITC-D permeability results showed that DSS increased the FITC-D permeability in the DSS group, compared with that of the vehical group (51.83 ± 2.48 vs 5.5 ± 1.05 , $P < 0.01$), while the administration of $1,25(\text{OH})_2\text{D}_3$ (10^{-9} M, 10^{-8} M, 10^{-7} M) afforded cytoprotection against DSS-induced monolayer hyper-permeability of Caco-2 cell monolayer (18.5 ± 1.05 vs 51.83 ± 2.48 , 8.17 ± 1.17 vs 51.83 ± 2.48 , 18.5 ± 1.05 vs 51.83 ± 2.48 , $P < 0.01$) in the $1,25(\text{OH})_2\text{D}_3$ -treated cells. Our data showed that $1,25(\text{OH})_2\text{D}_3$ (10^{-8} M) had a lower monolayer permeability to FITC-D when compared to that $1,25(\text{OH})_2\text{D}_3$ (10^{-9} M, 10^{-7} M). Therefore, the optimal concentration of $1,25(\text{OH})_2\text{D}_3$ on Caco-2 is 10^{-8} M for FITC-D permeability (Figure 5G). These data suggest that $1,25(\text{OH})_2\text{D}_3$ might help to maintain epithelial barrier integrity by preserving the expression of junction proteins and increase its resistance to DSS damage. These *in vitro* results are consistent with the observation *in vivo* that $1,25(\text{OH})_2\text{D}_3$ reduces DSS induced colitis in part by preserving TJ integrity of the epithelial mucosa.

Discussion

The intestinal mucosal integrity is a physical and metabolic barrier against toxins and pathogens in the lumen. The barrier regulates macromolecule trafficking between the lumen and the internal milieu and protects the host by preventing harmful solutes, microorganisms, toxins, and luminal antigens from entering the body [36]. Compromise in intestinal barrier function can result in an increased exposure of the host to luminal antigens and pathogens, leading to inflammation [37]. The epithelial

barrier function is largely determined by intercellular TJ. The TJ are responsible for restricting paracellular movement of compounds across the intestinal mucosa [38,39].

$1,25(\text{OH})_2\text{D}_3$ was found to protect the intestinal mucosa from various insults [40]. For example, $1,25(\text{OH})_2\text{D}_3$ may enhance defense mechanisms in the gastrointestinal mucosa and prevent mucosal injury in IBD [16]. In the present study, administration of $1,25(\text{OH})_2\text{D}_3$ was shown to ameliorate signs and symptoms of inflammation, such as colon shortening, weight loss, and increased DAI. Intestinal mucosa has crucial functions in regulating intestinal homeostasis by strictly protecting the subepithelial compartment from potentially noxious luminal compounds [41,42]. Kong et al. [6] have proved that vitamin D deficiency may compromise the mucosal barrier, leading to increased susceptibility to mucosal damage and increased risk of IBD. Intestinal barrier dysfunction is one of the major contributing factors in multiple pathological conditions of the gastrointestinal tract. An increased permeability in the TJ may provide a major site for both infection and establishment of inflammation in the gut [43-45]. Bacterial translocation is believed to occur via a paracellular pathway through the epithelial cells. Our data showed $1,25(\text{OH})_2\text{D}_3$ might have a protective effect on barrier integrity by maintaining the expression of TJ proteins, thereby reducing the severity of gut inflammation. This study adds to previous reports suggest that bioavailability of $1,25(\text{OH})_2\text{D}_3$ is an important contributing factor for determining the epithelial integrity.

Once the mucosal barrier is breached, the submucosa is exposed to a vast pool of luminal antigens, including food and bacteria, thereby engaging the innate immune responses including increased production in pro-inflammatory cytokines TNF- α and IFN- γ . We showed that the addition of $1,25(\text{OH})_2\text{D}_3$ was shown to ameliorate the DSS-induced high-expression in TNF- α and IFN- γ . The reduction in pro-inflammatory cytokines by $1,25(\text{OH})_2\text{D}_3$ may be either due to its direct suppressive effect on the expression of these pro-inflammatory cytokines or due to the effect on maintenance of epithelial barrier function, leading to a reduction in foreign luminal antigenic load, and a full activation of the innate immune system.

Conclusion

In summary, our data suggest that $1,25(\text{OH})_2\text{D}_3$ may be effective in ameliorating DSS-induced acute colitis, gauged by reducing clinical symptom, decreasing macroscopic and histological inflammation, enhancing epithelial cell resistance to injury and suppressing pro-inflammation responses to luminal antigens. Although some parts of the histology score are not obviously ameliorated by $1,25(\text{OH})_2\text{D}_3$, we think that there are

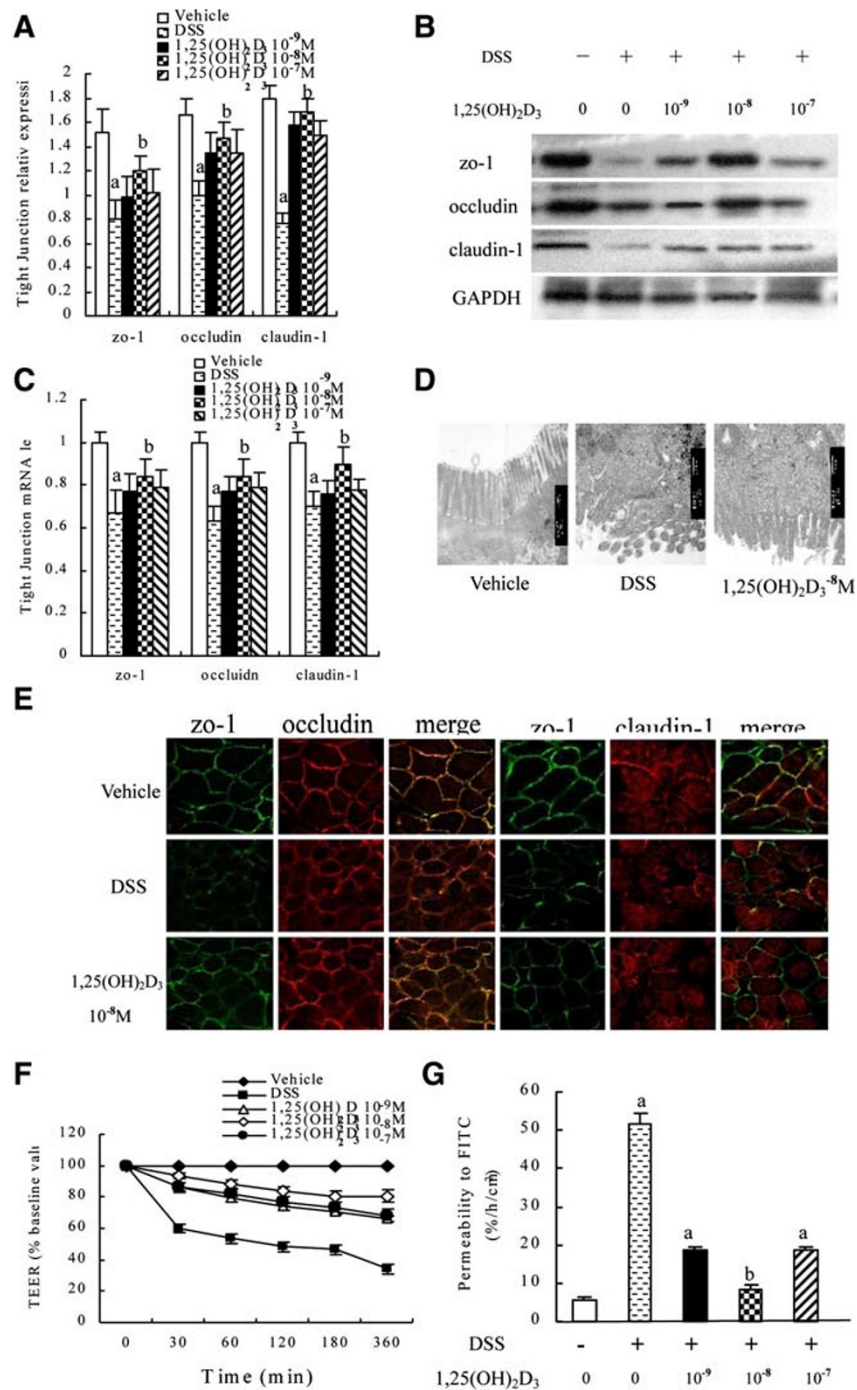


Figure 5 Effect of 1,25(OH)₂D₃ on the barrier function *in vitro*. (A and B) Induction of TJ proteins by 1,25(OH)₂D₃ in Caco-2 cells. Caco-2 cells were treated with indicated dose of 1,25(OH)₂D₃ for 48 h, and cell lysates were analyzed by Western blot. Western blot analysis showed induction of zo-1, occludin and claudin-1 proteins after 48 h of adding to 1,25(OH)₂D₃. (C) Expressions of zo-1, occludin, claudin-1 mRNA were assessed after adding to 1,25(OH)₂D₃ by real time Q-PCR. (D) TEM showed the disruption of the TJ, desmosomes, microvillus and brush border on the apical side of Caco-2 cell monolayer in the model group compared to that of the vehicle and 1,25(OH)₂D₃-treated group. (E) Cell monolayer was stained for occludin (red), claudin-1 (red) and zo-1 (green) by immunofluorescence staining, noting the disruption of the TJ and reduction of fluorescence intensity in DSS group. (F) Effect of 1,25(OH)₂D₃ on TEER. A dose-dependent recovery of TEER with 1,25(OH)₂D₃-treated was seen. (G) Paracellular FITC-D was measured with or without 2% DSS in the absence or presence of 1,25(OH)₂D₃ at 10⁻⁹, 10⁻⁸, 10⁻⁷ M (administered 2 h prior to DSS) for 48 h, 1,25(OH)₂D₃ attenuated the epithelial hyperpermeability induced by DSS. Data were expressed as mean ± SD. ^aP < 0.05 vs vehicle group, ^bP < 0.05 vs DSS group.

some reasons, such as: a short treatment time, a very slow process of pathological change and so on. However, the effect of 1,25(OH)₂D₃ in IBD is worth further study. Our data showed that 1,25(OH)₂D₃ may play an important role in maintaining epithelial integrity and regulating the innate immune responses. The therapeutic potential of 1,25(OH)₂D₃ for the treatment of human colitis warrants exploration.

Competing interests

The authors declare that they have no competing interests. This work was supported by public health bureau grant of Hebei province (No. 20090104) to XL Zhang. Non-financial competing interests. Non-patents competing interests. Non-any stocks or shares in an organization.

Authors' contributions

HZ, HZ and HW participated in the design of the study and performed the statistical analysis and drafted the manuscript. HL and LL conceived of the study; JG and CL collected of data and analyzed histological scores; XZ and DQS participated in its design and coordination, helped to draft the manuscript and have given final approval of the version to be published. All authors read and approved the final manuscript.

Acknowledgements

The authors gratefully acknowledge the financial support from strong, characteristic discipline and public health bureau grant of Hebei province to XL Zhang (No. 20090104) and from the second hospital of Hebei Medical University fund to L LIU (No.2 h0201114). We thank all members of the Hebei key laboratory of gastroenterology for their contributions to this work and Bo Shen M.D. (Professor of Medicine, Department of Gastroenterology & Hepatology, Cleveland Clinic) for critical reading of the manuscript. The authors are grateful to Yanping Cao (Department of pathology, Hebei Medical University, Shijiazhuang, Hebei, China) for analyzing histological scores and Keling Wang (Department of psychiatry, Children's Hospital of Hebei Province, Shijiazhuang, Hebei, China) for her excellent technical assistance.

Author details

¹Department of Gastroenterology, The Second Hospital of Hebei Medical University, Hebei Key Laboratory of Gastroenterology, Hebei Institute of Gastroenterology, No.215 Heping West Road, 050000 Shijiazhuang, China. ²Hebei Medical University, No.361 Zhongshan East Road, 050017 Shijiazhuang, China. ³Inflammatory Bowel & Immunobiology Research Institute, Cedars-Sinai Medical Center, Los Angeles, CA 90048, USA.

Received: 4 February 2012 Accepted: 15 April 2012

Published: 30 May 2012

References

1. Aoyagi Y, Nagata S, Kudo T, Fujii T, Wada M, Chiba Y, Ohtsuka Y, Yamashiro Y, Shimizu T, Ohkusa T: Peroxisome proliferator-activated receptor gamma 2 mutation may cause a subset of ulcerative colitis. *Pediatr Int* 2010, **52**:729–734.
2. Matricon J, Barnich N, Ardid D: Immunopathogenesis of inflammatory bowel disease. *Self Nonself* 2010, **1**:299–309.
3. Gibson PR: Increased gut permeability in Crohn's disease: is TNF the link? *Gut* 2004, **53**:1724–1725.
4. McGuckin MA, Eri R, Simms LA, Florin TH, Radford-Smith G: Intestinal barrier dysfunction in inflammatory bowel diseases. *Inflamm Bowel Dis* 2009, **15**:100–113.
5. Turner JR: Intestinal mucosal barrier function in health and disease. *Nat Rev Immunol* 2009, **9**:799–809.
6. Hering NA, Schulzke JD: Therapeutic options to modulate barrier defects in inflammatory bowel disease. *Dig Dis* 2009, **27**:450–454.
7. Koch S, Nusrat A: Dynamic regulation of epithelial cell fate and barrier function by intercellular junctions. *Ann N Y Acad Sci* 2009, **1165**:220–227.
8. Naydenov NG, Hopkins AM, Ivanov AI: c-Jun N-terminal kinase mediates disassembly of apical junctions in model intestinal epithelia. *Cell Cycle* 2009, **8**:2110–2121.
9. Hashimoto K, Oshima T, Tomita T, Kim Y, Matsumoto T, Joh T, Miwa H: Oxidative stress induces gastric epithelial permeability through claudin-3. *Biochem Biophys Res Commun* 2008, **376**:154–157.
10. Diesing AK, Nossol C, Panther P, Walk N, Post A, Klues J, Kreutzmann P, Danicke S, Rothkotter HJ, Kahlert S: Mycotoxin deoxynivalenol (DON) mediates biphasic cellular response in intestinal porcine epithelial cell lines IPEC-1 and IPEC-J2. *Toxicol Lett* 2011, **200**:8–18.
11. Ewert P, Aguilera S, Alliende C, Kwon YJ, Albornoz A, Molina C, Urzua U, Quest AF, Olea N, Perez P, Castro I, Barrera MJ, Romo R, Hermoso M, Leyton C, Gonzalez MJ: Disruption of tight junction structure in salivary glands from Sjogren's syndrome patients is linked to proinflammatory cytokine exposure. *Arthritis Rheum* 2010, **62**:1280–1289.
12. Severson EA, Kwon M, Hilgarth RS, Parkos CA, Nusrat A: Glycogen Synthase Kinase 3 (GSK-3) influences epithelial barrier function by regulating occludin, claudin-1 and E-cadherin expression. *Biochem Biophys Res Commun* 2010, **397**:592–597.
13. Fillon S, Robinson ZD, Colgan SP, Furuta GT: Epithelial function in eosinophilic gastrointestinal diseases. *Immunol Allergy Clin North Am* 2009, **29**:171–178.
14. George MD, Wehkamp J, Kays RJ, Leutenegger CM, Sabir S, Grishina I, Dandekar S, Bevins CL: In vivo gene expression profiling of human intestinal epithelial cells: analysis by laser microdissection of formalin fixed tissues. *BMC Genomics* 2008, **9**:209.
15. Ramakrishna BS: Probiotic-induced changes in the intestinal epithelium: implications in gastrointestinal disease. *Trop Gastroenterol* 2009, **30**:76–85.
16. Laverny G, Penna G, Vetrano S, Correale C, Nebuloni M, Danese S, Adorini L: Efficacy of a potent and safe vitamin D receptor agonist for the treatment of inflammatory bowel disease. *Immunol Lett* 2010, **131**:49–58.
17. Bruce D, Yu S, Ooi JH, Cantorna MT: Converging pathways lead to overproduction of IL-17 in the absence of vitamin D signaling. *Int Immunol* 2011, **23**:519–528.
18. Ardizzone S, Cassinotti A, Bevilacqua M, Clerici M, Porro GB: Vitamin D and inflammatory bowel disease. *Vitam Horm* 2011, **86**:367–377.
19. Kong J, Zhang Z, Musch MW, Ning G, Sun J, Hart J, Bissonnette M, Li YC: Novel role of the vitamin D receptor in maintaining the integrity of the intestinal mucosal barrier. *Am J Physiol Gastrointest Liver Physiol* 2008, **294**:208–216.
20. von Essen MR, Kongsbak M, Schjerling P, Olgaard K, Odum N, Geisler C: Vitamin D controls T cell antigen receptor signaling and activation of human T cells. *Nat Immunol* 2010, **11**:344–349.
21. Sun J: Vitamin D and mucosal immune function. *Curr Opin Gastroenterol* 2010, **26**:591–595.
22. Froicu M, Cantorna MT: Vitamin D and the vitamin D receptor are critical for control of the innate immune response to colonic injury. *BMC Immunol* 2007, **8**:5.
23. Froicu M, Weaver V, Wynn TA, McDowell MA, Welsh JE, Cantorna MT: A crucial role for the vitamin D receptor in experimental inflammatory bowel diseases. *Mol Endocrinol* 2003, **17**:2386–2392.
24. Kamen DL, Tangpricha V: Vitamin D and molecular actions on the immune system: modulation of innate and autoimmunity. *J Mol Med* 2010, **88**:441–450.
25. Cantorna MT: Mechanisms underlying the effect of vitamin D on the immune system. *Proc Nutr Soc* 2010, **69**:286–289.
26. Adams JS, Hewison M: Update in vitamin D. *J Clin Endocrinol Metab* 2010, **95**:471–478.
27. Onsonby AL, Lucas RM, van der Mei IA: UVR, vitamin D and three autoimmune diseases—multiple sclerosis, type 1 diabetes, rheumatoid arthritis. *Photochem Photobiol* 2005, **81**:1267–1275.
28. Goertz B, Fassbender WJ, Williams JC, Marzeion AM, Bretzel RG, Stracke H, Berliner MN: Vitamin D receptor genotypes are not associated with rheumatoid arthritis or biochemical parameters of bone turnover in German RA patients. *Clin Exp Rheumatol* 2003, **21**:333–339.
29. Cantorna MT, Munsick C, Bemiss C, Mahon BD: 1,25-Dihydroxycholecalciferol prevents and ameliorates symptoms of experimental murine inflammatory bowel disease. *J Nutr* 2000, **130**:2648–2652.
30. Cooper HS, Murthy SN, Shah RS, Sedergran DJ: Clinicopathologic study of dextran sulfate sodium experimental murine colitis. *Lab Invest* 1993, **69**:238–249.

31. Shimizu T, Suzuki T, Yu HP, Yokoyama Y, Choudhry MA, Bland KI, Chaudry IH: **The role of estrogen receptor subtypes on hepatic neutrophil accumulation following trauma-hemorrhage: direct modulation of CINC-1 production by Kupffer cells.** *Cytokine* 2008, **43**:88–92.
32. Nygaard UC, Hansen JS, Samuelsen M, Alberg T, Marioara CD, Løvik M: **Single-walled and multi-walled carbon nanotubes promote allergic immune responses in mice.** *Toxicol Sci* 2009, **109**:113–123.
33. Plevy SE, Landers CJ, Prehn J, Carramanzana NM, Deem RL, Shealy D, Targan SR: **A role for TNF-alpha and mucosal T helper-1 cytokines in the pathogenesis of Crohn's disease.** *J Immunol* 1997, **159**:6276–6282.
34. Nagy JA, Herzberg KT, Masse EM, Zientara GP, Dvorak HF: **Exchange of macromolecules between plasma and peritoneal cavity in ascites tumor-bearing, normal, and serotonin-injected mice.** *Cancer Res* 1989, **49**:5448–5458.
35. Tschugguel W, Zhegu Z, Gajdzik L, Maier M, Binder BR, Graf J: **High precision measurement of electrical resistance across endothelial cell monolayers.** *Pflügers Arch* 1995, **430**:145–147.
36. Park EJ, Thomson AB, Clandinin MT: **Protection of intestinal occludin tight junction protein by dietary gangliosides in lipopolysaccharide-induced acute inflammation.** *J Pediatr Gastroenterol Nutr* 2010, **50**:321–328.
37. Chichlowski M, Westwood GS, Abraham SN, Hale LP: **Role of mast cells in inflammatory bowel disease and inflammation-associated colorectal neoplasia in IL-10-deficient mice.** *PLoS One* 2010, **17**:e12220.
38. McCall IC, Betanzos A, Weber DA, Nava P, Miller GW, Parkos CA: **Effects of phenol on barrier function of a human intestinal epithelial cell line correlate with altered tight junction protein localization.** *Toxicol Appl Pharmacol* 2009, **241**:61–70.
39. Suzuki T, Yoshinaga N, Tanabe S: **IL-6 regulates claudin-2 expression and tight junction permeability in intestinal epithelium.** *J Biol Chem* 2011, Jul 19 M111.238147.
40. Johnson CS, Muindi JR, Hershberger PA, Trump DL: **The antitumor efficacy of calcitriol: preclinical studies.** *Anticancer Res* 2006, **26**:2543–2549.
41. McKenna LB, Schug J, Vourekas A, McKenna JB, Bramswig NC, Friedman JR, Kaestner KH: **MicroRNAs control intestinal epithelial differentiation, architecture, and barrier function.** *Gastroenterology* 2010, **139**:1654–1664.
42. Mayol JM, Adame-Navarrete Y, Alarma-Estrany P, Molina-Roldan E, Huete-Toral F, Fernandez-Represa JA: **Luminal oxidants selectively modulate electrogenic ion transport in rat colon.** *World J Gastroenterol* 2006, **12**:5523–5527.
43. Ohira M, Oshitani N, Hosomi S, Watanabe K, Yamagami H, Tominaga K, Watanabe T, Fujiwara Y, Maeda K, Hirakawa K, Arakawa T: **Dislocation of Rab13 and vasodilator-stimulated phosphoprotein in inactive colon epithelium in patients with Crohn's disease.** *Int J Mol Med* 2009, **24**:829–835.
44. Oshitani N, Watanabe K, Nakamura S, Fujiwara Y, Higuchi K, Arakawa T: **Dislocation of tight junction proteins without F-actin disruption in inactive Crohn's disease.** *Int J Mol Med* 2005, **15**:407–410.
45. Qin H, Zhang Z, Hang X, Jiang Y: **L. plantarum prevents enteroinvasive Escherichia coli-induced tight junction proteins changes in intestinal epithelial cells.** *BMC Microbiol* 2009, **9**:63.

doi:10.1186/1471-230X-12-57

Cite this article as: Zhao et al.: Protective role of 1,25(OH)₂vitamin D₃ in the mucosal injury and epithelial barrier disruption in DSS-induced acute colitis in mice. *BMC Gastroenterology* 2012 **12**:57.

Submit your next manuscript to BioMed Central and take full advantage of:

- Convenient online submission
- Thorough peer review
- No space constraints or color figure charges
- Immediate publication on acceptance
- Inclusion in PubMed, CAS, Scopus and Google Scholar
- Research which is freely available for redistribution

Submit your manuscript at
www.biomedcentral.com/submit

